JACS
JOURNAL OF THE AMERICAN CHEMICAL SOCIETY

Communication

pubs.acs.org/JACS

Prato Reaction of $M_3N@I_h$-C_{80} (M = Sc, Lu, Y, Gd) with Reversible Isomerization

Safwan Aroua and Yoko Yamakoshi*

Laboratorium für Organische Chemie, ETH-Zürich, Wolfgang-Pauli-Strasse 10, CH-8093 Zürich, Switzerland.

Supporting Information

ABSTRACT: The 1,3-dipolar cycloaddition of an azomethine ylide (Prato reaction) with $M_3N@I_h$-C_{80} (denoted as $M_3N@C_{80}$; M = Sc, Lu, Y, Gd) was carried out to obtain fulleropyrrolidinebis(carboxylic acid) derivatives as scaffolds for the preparation of various functionalized $M_3N@C_{80}$ materials. The formation of two monoadduct isomers (the [6,6]- and [5,6]-adducts) were detected by HPLC and identified by NMR and vis/NIR spectroscopies. In each Prato reaction with $M_3N@C_{80}$, the initial addition gave a [6,6]-adduct of the I_h-C_{80} cage, and subsequently, a [5,6]-adduct was obtained by complete or partial thermal isomerization via a rearrangement reaction. The reaction rate of the latter thermal conversion of the adducts was dependent on the size of the metal cluster inside C_{80}, and interestingly, in the reactions of $Y_3N@C_{80}$ and $Gd_3N@C_{80}$, this conversion was found to be reversible for the first time. Detailed kinetic studies provided the enthalpy and entropy barriers for the reactions of the adducts of $Lu_3N@C_{80}$, $Y_3N@C_{80}$, and $Gd_3N@C_{80}$. The utility of the obtained Prato adducts was confirmed by preparation of a highly water-soluble $Gd_3N@C_{80}$ derivative.

The high-yielding syntheses of trimetallic nitride template endohedral metallofullerenes (TNT-EMFs),[1] $M_3N@I_h$-C_{80} (denoted as $M_3N@C_{80}$), have stimulated the production of new potential materials for MRI contrast agents[2] and solar cells.[3] Our interest has been focused on the applications of fullerenes as biomaterials, taking advantage of their photosensitivity[4,5] and metal encapsulation of paramagnetic metals such as Gd^{3+}.[6,7] For the production of new materials, it is important to identify useful scaffold derivatives for the preparation of devices and probes requiring water-soluble materials. In the present study, we chose the Prato reaction,[8] which is widely used for chemical functionalization of C_{60} because of its operational simplicity and high yield, to prepare fulleropyrrolidinebis(carboxylic acid) derivative of $Gd_3N@C_{80}$ with ^{t}Bu protection. Simultaneously, $Sc_3N@C_{80}$ was subjected to the same Prato reaction to analyze the detailed structure of the adducts by NMR spectroscopy. The unexpected difference in the regioselectivities of the reactions with $Sc_3N@C_{80}$ and $Gd_3N@C_{80}$ following initial addition and subsequent thermal isomerization prompted us to conduct further experiments with $Lu_3N@C_{80}$ and $Y_3N@C_{80}$ to investigate how the reaction depends on the metal cluster in the C_{80} cage (Figure 1). Interestingly, we found that the thermal conversions from the initial kinetic [6,6]-adducts to the thermodynamically stable [5,6]-adducts for $Gd_3N@C_{80}$ and $Y_3N@C_{80}$ are reversible.

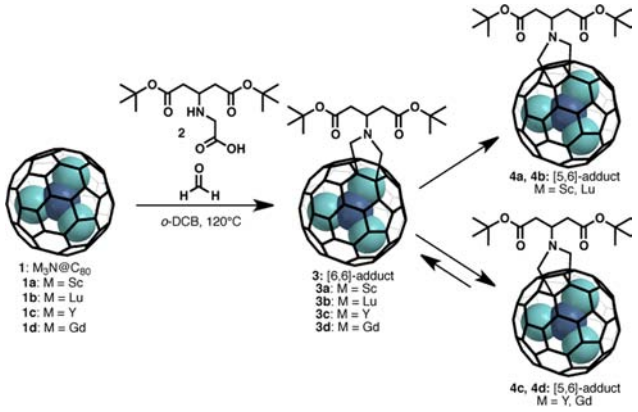

Figure 1. Prato reaction of $M_3N@I_h$-C_{80} **1a–d** (M = Sc, Lu, Y, Gd, respectively) with glycine derivative **2** and formaldehyde to provide [6,6]- and [5,6]-monoadducts (**3a–d** and **4a–d**, respectively) with two carboxylic acid ester groups. The positions and angles of the M_3N inside the cage are random.

The groups of Dorn and Echegoyen intensively studied the regioselectivity of the Prato adducts of $M_3N@C_{80}$. In I_h-C_{80}, there are two possible addition sites for the Prato reaction: the [6,6]-junction (a bond at the border of two hexagons; adducts **3a–d** in Figure 1) and the [5,6]-junction (a bond at the border of a pentagon and a hexagon; adducts **4a–d** in Figure 1). Their initial reports showed that $Sc_3N@C_{80}$ provides the [5,6]-adduct while $Y_3N@C_{80}$ provides the [6,6]-adduct,[9−11] and further studies indicated that the [6,6]-adducts are kinetic products, which are subsequently converted to the thermodynamically stable [5,6]-adducts upon heating.[12−14] In addition, Lu and coworkers used HPLC analysis to show that the [6,6]-adduct is the thermodynamic product in the Prato reaction of $Gd_3N@C_{80}$.[15]

In the present study, we subjected the new glycine derivative **2** to the Prato reaction with formaldehyde to obtain fulleropyrrolidinebis(carboxylic acid) derivatives **3** and **4** (Figure 1) as precursors for the preparation of functionalized fullerene materials. Previously, carboxylic acid derivatives of $M_3N@C_{80}$ (M = Lu, Y, Gd) were prepared by Hirsch−Bingel reactions.[11,16,17] This proved difficult with $Sc_3N@C_{80}$[11] but was accomplished by the addition of *N*,*N*-dimethylformamide (DMF).[18] Here we used the Prato reaction and obtained monoadducts of $Sc_3N@C_{80}$ as determined by HPLC (peaks **A**

Received: September 26, 2012
Published: December 4, 2012

   dx.doi.org/10.1021/ja309550z | *J. Am. Chem. Soc.* 2012, 134, 20242−20245

and **B** in Figure 2a). Monoadduct **A**, which was obtained as the final product,[19] was purified and identified as the [5,6]-adduct by

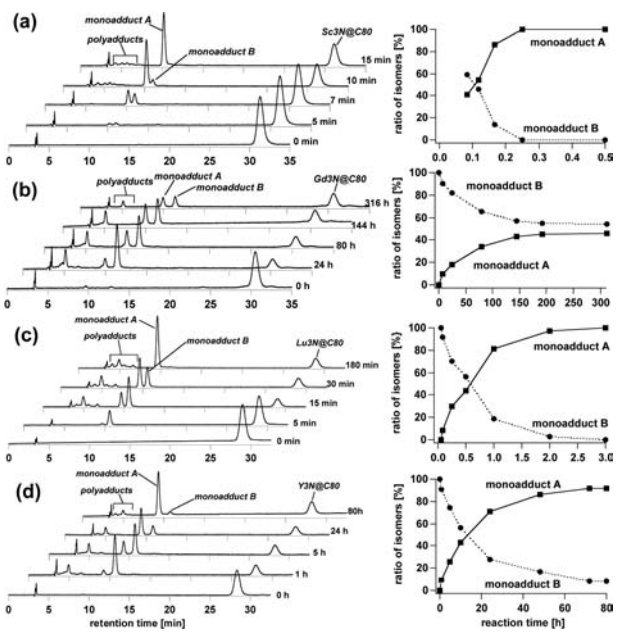

Figure 2. Generation of Prato monoadducts **A** and **B** of (a) $Sc_3N@C_{80}$, (b) $Gd_3N@C_{80}$, (c) $Lu_3N@C_{80}$ (c), and (d) $Y_3N@C_{80}$ monitored by HPLC (Buckyprep, 4.6 mm i.d. × 250 mm, toluene, 1 mL/min, 390 nm). In each reaction, **A** was identified as the [5,6]-adduct and **B** as the [6,6]-adduct by NMR and vis/NIR analyses of the isolated products (see Figures 3 and 4).

NMR spectroscopy.[20] The same reaction of $Gd_3N@C_{80}$, however, initially provided adduct **B**, which slowly interconverted to **A** (Figure 2b). This latter thermal conversion of $Gd_3N@C_{80}$ adducts was much slower than that with $Sc_3N@C_{80}$ and did not reach completion after >300 h (Figure 2b). Adducts **A** and **B** of $Gd_3N@C_{80}$ were not identified by NMR analysis because of their paramagnetic property.

The same Prato reactions were carried out on $Lu_3N@C_{80}$ and $Y_3N@C_{80}$ having medium-sized M^{3+} ions ($Gd^{3+} > Y^{3+} > Lu^{3+} > Sc^{3+}$) (Figure 2c,d). The monoadducts **A** and **B** were purified and assigned as [5,6]- and [6,6]-adducts, respectively, by NMR analysis. For instance, as shown in Figure 3, the adducts of $Lu_3N@C_{80}$ were assigned on the basis of two different mirror symmetries, which provided different peak patterns in both the ^1H and ^{13}C NMR spectra. On the basis of the structural identification of the [5,6]- and [6,6]-adducts of $M_3N@C_{80}$ (M = Sc, Lu, Y) by NMR analysis, the two adducts of $Gd_3N@C_{80}$ (peaks **A** and **B** in Figure 2b) were identified as **4d** and **3d** by comparing their vis/NIR spectra with unique absorbance pattern for each adduct (Figure 4). All of the [6,6]-adducts have three absorbance peaks between 620 and 850 nm (Figure 4a), and all of the [5,6]-adducts have a single absorbance peak at 830−970 nm (λ_{max} = 970, 860, 830, and 860 nm for **4a**−**d**, respectively; Figure 4b).[11,21] Interestingly, the peak for the [5,6]-adduct of $Sc_3N@C_{80}$ was more red-shifted than those for the other $M_3N@C_{80}$ [5,6]-adducts, indicating a smaller band gap, presumably resulting from a lower LUMO level (Table 1). The patterns of the bands between 700 and 850 nm for the [6,6]-adducts were dependent on the metal cluster size. In addition, the HPLC retention times (t_R) of the [5,6]-adducts were shorter than those

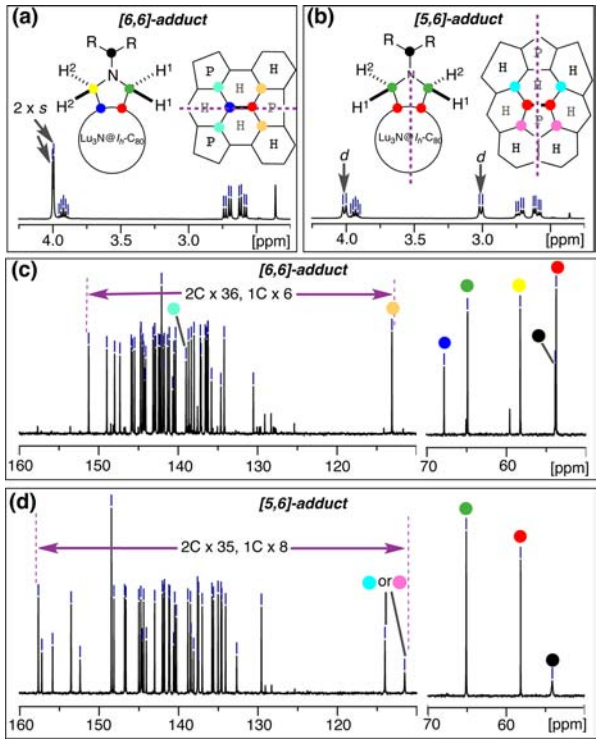

Figure 3. Structural identification of adducts (a, c) **B** and (b, d) **A** of $Lu_3N@C_{80}$ by NMR analysis. Because of the different mirror symmetries of the C_{80} parts of the two adducts, the pyrrolidine methylene protons (H^1 and H^2) appear as two singlets for the [6,6]-adduct (a) and as two doublets for the [5,6]-adduct (b). In the ^{13}C NMR spectrum, each pyrrolidine methylene carbon and each sp^3 carbon in the C_{80} cage gives rise to two separate signals for the [6,6]-adduct (c) but only one signal for the [5,6]-adduct (d). The aromatic region in the ^{13}C NMR spectrum of the [6,6]-adduct showed 36 peaks integrating to 2C and six peaks integrating to 1C, while the [5,6]-adduct showed 35 2C peaks and eight 1C peaks. By HMQC and HMBC analyses, the sp^2 carbons adjacent to the sp^3 carbons were assigned in the ^{13}C NMR spectra.[22]

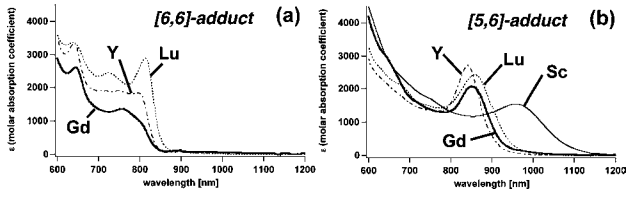

Figure 4. Vis/NIR absorption spectra of the (a) [6,6]- and (b) [5,6]-adducts of $M_3N@C_{80}$ (measured in 0.5 mg/mL solutions in toluene and normalized as the molar absorption coefficients ε). The [6,6]-adduct of $Sc_3N@C_{80}$ could not be isolated because conversion to the [5,6]-adduct was too rapid.

of the [6,6]-adducts for all of the $M_3N@C_{80}$, and the difference was related to the size of the cluster (Table 1).

Consistent with the previous studies[12,14] these results show that the [6,6]-adducts were observed as the initial major adducts (kinetic product) and the [5,6]-adducts as the thermodynamically more stable products. In general, the reactivity of the initial addition to the double bond of C_{80} is related to (1) the electron density caused by charge transfer from M_3N to C_{80}, (2) the steric effect due to pyramidalization of the C_{80} cage carbons by the M_3N cluster, and (3) the redox potentials, which are dependent on the metal in M_3N. The pyramidalization effects on carbons at

dx.doi.org/10.1021/ja309550z | J. Am. Chem. Soc. 2012, 134, 20242−20245

Table 1. Properties of $M_3N@C_{80}$ in the Prato Reaction

property		M^{3+} in $M_3N@C_{80}$			
		Sc^{3+}	Lu^{3+}	Y^{3+}	Gd^{3+}
ionic radius (Å)		0.75	0.85	0.90	0.94
Pauling electronegativity		1.36	1.27	1.22	1.20
$M_3N@C_{80}$ redox potentials (V)	E_{red}	−1.26	−1.40	−1.41	−1.44
	E_{ox}	0.59	0.64	0.64	0.58
E_{red} of [6,6]-adduct (V)[a]		–	−1.23	−1.28	−1.27
E_{red} of [5,6]-adduct (V)[a]		−1.06	−1.14	−1.17	−1.20
optical band gap (eV)[b]	[6,6]-adduct	–	1.31	1.36	1.34
	[5,6]-adduct	1.13	1.42	1.46	1.46
chemical shift(s) of sp^3 carbons at the addition site (ppm)	[6,6]-adduct (PHHJ/THJ)	−/−	53.89/67.84	57.67/67.96	−/−
	[5,6]-adduct (PHHJ)	57.25	58.18	59.30	–
difference in HPLC t_R for the [5,6]- and [6,6]-adducts (min)		0.81	0.90	1.41	1.43
total yield of monoadducts (%)[c]		45	56	56	57
time for 50% conversion from [6,6]- to [5,6]-adduct (min)[d]		7	20−25	600	18000
final [6,6]:[5,6] ratio[d]		0:100	0:100	7:93	50:50
isomerization barriers[d]	$\Delta H^{\ddagger}$ (kJ/mol)	–	98.5	114.5	119.5
	$\Delta S^{\ddagger}$ (J K^{-1} mol^{-1})	–	−62.5	−49.0	−55.0

[a]Measured by differential pulse voltammetry on a 1 mm glassy-carbon disk electrode in *o*-dichlorobenzene (*o*-DCB) with 0.05 M tetrabutylammonium hexafluorophosphate, scan rate 20 mV/s, pulse amplitude 50 mV, pulse width 50 mV. All of the potentials were corrected relative to ferrocene as an internal standard (V vs $Fc^0/^+$).[30] [b]Measured in toluene. [c]Estimated from the HPLC peak areas obtained after 15 min of reaction. [d]Estimated by HPLC analysis.[25]

three-hexagon junctions (THJs) of $M_3N@C_{80}$ (M = Sc, Lu, Y) by the metal cluster were reported by Dunsch and co-workers to depend on the size[23] and the geometry[1,24−26] of the M_3N cluster on the basis of the ^{13}C NMR chemical shift of the sp^2 carbons. However, in the present study, we did not see any significant difference in the reaction rate of the initial addition.

Instead, large differences in the rates of the subsequent thermal isomerizations were observed for $M_3N@C_{80}$ with different metal clusters, with larger cluster sizes leading to lower reaction rates. We speculated that a larger metal cluster contributes more to the stabilization of the [6,6]-adduct via the pyramidalization of the sp^3 carbons at the [6,6]-junction. Consistently, the signal of the sp^3 carbons at pentagon−hexagon−hexagon junctions (PHHJs) was significantly shifted downfield in the adduct of M = Y (57.7 ppm) relative to M = Lu (53.9 ppm) (Table 1). The effect of the size of the metal cluster was also investigated by Lu and co-workers through a comparison of the regioselectivity of Prato reactions of $Gd_3N@C_{80}$ with $Sc_xGd_{3-x}@C_{80}$ (x = 0−3), which showed that $Gd_3N@C_{80}$ with largest metal cluster provided the [6,6]-adduct in good agreement with the calculated energy of the adducts.[15] The time scale of the isomerization step in our Prato reaction with $Sc_3N@C_{80}$ seems to be much shorter (within 15 min at 120 °C) than that for *N*-tritylfulleropyrrolidine[14,27] but longer than those for *N*-methyl- and *N*-ethylfulleropyrrolidine.[9,10,12] More importantly, while the isomerizations of the $Sc_3N@C_{80}$ and $Lu_3N@C_{80}$ adducts reached completion, the thermal conversions of the $Y_3N@C_{80}$ and $Gd_3N@C_{80}$ adducts did not, and a certain amount of the [6,6]-adducts remained in the reaction mixtures (7 and 50%,[28] respectively), indicating that these isomers were in equilibrium.

To confirm the reversibility of the thermal conversion of the adducts of $Y_3N@C_{80}$ and $Gd_3N@C_{80}$, each of the purified adducts was subjected to heating. After 4 h of heating at 180 °C, the two reaction mixtures contained identical [6,6]/[5,6] product ratios, as analyzed by HPLC. Figure 5 shows the results using the pure adducts of $Gd_3N@C_{80}$, which provided a 50:50 **3d**/**4d** ratio after thermal treatment.[28] This clearly confirmed that the isomerization reached equilibrium.[29] In the thermal

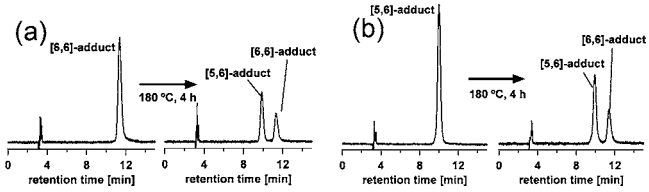

Figure 5. Thermal conversions of (a) the $Gd_3N@C_{80}$ [6,6]-adduct to the [5,6]-adduct (**3d** to **4d**) and (b) the [5,6]-adduct to the [6,6]-adduct (**4d** to **3d**) upon heating at 180 °C for 4 h as monitored by HPLC (Buckyprep, 4.6 mm i.d. × 250 mm, toluene, 1 mL/min, 390 nm).[28]

conversions of the pure [6,6]- and [5,6]-adducts of $Y_3N@C_{80}$, a **3c**/**4c** ratio of 7:93 was obtained (Figure S31 in the Supporting Information). These results indicate that the energy levels of the [5,6]- and [6,6]-adducts of $Y_3N@C_{80}$ or $Gd_3N@C_{80}$ are similar, in contrast to the adducts of $Sc_3N@C_{80}$ and $Lu_3N@C_{80}$. In the previous studies, reversible isomerization of the Prato adducts was not observed for $M_3N@C_{80}$ (M = Y[12] and Gd[15]). We speculate that the carbonyl group may help to stabilize the high-energy intermediate in our adducts. To estimate the activation enthalpies and entropies, the isomerization reactions were carried out at various temperatures, and Eyring plots were constructed.[20] The enthalpy barrier for isomerization ([6,6]-adduct to [5,6]-adduct) was found to increase with increasing cluster size (Table 1).

The previous reports on exohedral functionalization of $M_3N@C_{80}$ with X-ray crystal structures showed that the sp^2 carbons adjacent to the sp^3 carbons at the addition site were the most flattened carbons in the C_{80} cage.[21,25] In the present study, on the basis of the ^{13}C NMR shift, we observed that the PHHJ sp^2 carbons adjacent to the THJ sp^3 carbons in the [6,6]-adduct were less flattened (e.g., 139 ppm in Figure 3c), which may explain the instability of the [6,6]-adducts. Further studies involving X-ray crystal structure analysis of the adducts will explain more clearly the relationship between carbon pyramidalization and adduct stability.

dx.doi.org/10.1021/ja309550z | J. Am. Chem. Soc. 2012, 134, 20242−20245

To evaluate the utility of these fulleropyrrolidine derivatives as scaffolds for further functionalization, a coupling reaction was carried out (Figure 6). Deprotection of the ^{t}Bu groups was

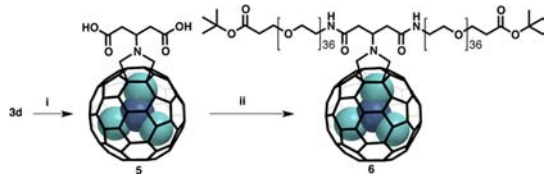

Figure 6. Preparation of a water-soluble $Gd_3N@C_{80}$ derivative by the addition of PEG chains. Conditions: (i) 1:1 TFA/$CHCl_3$, 18 h, 100%; (ii) $NH_2(CH_2CH_2O)_{36}CH_2CH_2COO^tBu$, HBTU, DIPEA, 1:1 DMF/*o*-DCB, rt, 4 days, 77%.

successfully carried out under acidic conditions. Subsequent coupling reactions using HBTU provided poly(ethylene glycol) (PEG) derivative **6**, which possess high water solubility (>3 mM). The physical properties of water-soluble **6** (e.g., r_1 relaxivity and photosensitivity) are under investigation.

In summary, Prato reactions of $M_3N@C_{80}$ (M = Sc, Lu, Y, Gd) using a new azomethine ylide provided bis(carboxylic acid) derivatives. A kinetic study of the regioselective generation of adducts indicated that the initial 1,3-dipolar addition occurred at a [6,6]-junction and was followed by thermal rearrangement to a [5,6]-junction. When $M_3N@C_{80}$ (M = Y, Gd) was used, this rearrangement reaction occurred reversibly. It appears that the kinetics of isomerization and the stabilities of the two isomers are highly related to the size of the metal cluster inside the C_{80} cage. We speculate that the difference between the reaction rates for thermal rearrangement reported here and those previously reported for fulleropyrrolidine derivatives of $M_3N@C_{80}$ is related to the bulkiness of the substitutent group connected to the N atom and that the carbonyl groups may play a key role in stabilizing the intermediate. Further investigations involving X-ray structure analysis and theoretical calculations are needed to fully understand the process.

■ ASSOCIATED CONTENT

Ⓢ Supporting Information

Synthesis details and characterization data for all $M_3N@C_{80}$ compounds. This material is available free of charge via the Internet at http://pubs.acs.org.

■ AUTHOR INFORMATION

Corresponding Author

yamakoshi@org.chem.ethz.ch

Notes

The authors declare no competing financial interest.

■ ACKNOWLEDGMENTS

The authors thank Prof. Grüzmacher and Dr. Schönberg in the Laboratory of Inorganic Chemistry of ETH-Zürich for their help on electrochemical measurements. This study was supported in part by the American Heart Association (0930140N to Y.Y.), the PRESTO Program of the Japan Science and Technology Agency (Y.Y.), and an ETH Individual Investigator's Research Award (Y.Y.).

■ REFERENCES

(1) Stevenson, S.; Rice, G.; Glass, T.; Harich, K.; Cromer, F.; Jordan, M. R.; Craft, J.; Hadju, E.; Bible, R.; Olmstead, M. M.; Maitra, K.; Fisher, A. J.; Balch, A. L.; Dorn, H. C. *Nature* **1999**, *402*, 898.
(2) Zhang, J. F.; Fatouros, P. P.; Shu, C. Y.; Reid, J.; Owens, L. S.; Cai, T.; Gibson, H. W.; Long, G. L.; Corwin, F. D.; Chen, Z. J.; Dorn, H. C. *Bioconjugate Chem.* **2010**, *21*, 610.
(3) Ross, R. B.; Cardona, C. M.; Guldi, D. M.; Sankaranarayanan, S. G.; Reese, M. O.; Kopidakis, N.; Peet, J.; Walker, B.; Bazan, G. C.; Van Keuren, E.; Holloway, B. C.; Drees, M. *Nat. Mater.* **2009**, *8*, 208.
(4) Yamakoshi, Y.; Sueyoshi, S.; Fukuhara, K.; Miyata, N. *J. Am. Chem. Soc.* **1998**, *120*, 12363.
(5) Yamakoshi, Y.; Umezawa, N.; Ryu, A.; Arakane, K.; Miyata, N.; Goda, Y.; Masumizu, T.; Nagano, T. *J. Am. Chem. Soc.* **2003**, *125*, 12803.
(6) Mikawa, M.; Kato, H.; Okumura, M.; Narazaki, M.; Kanazawa, Y.; Miwa, N.; Shinohara, H. *Bioconjugate Chem.* **2001**, *12*, 510.
(7) Bolskar, R. D.; Benedetto, A. F.; Husebo, L. O.; Price, R. E.; Jackson, E. F.; Wallace, S.; Wilson, L. J.; Alford, J. M. *J. Am. Chem. Soc.* **2003**, *125*, 5471.
(8) Maggini, M.; Scorrano, G.; Prato, M. *J. Am. Chem. Soc.* **1993**, *115*, 9798.
(9) Cardona, C. M.; Kitaygorodskiy, A.; Ortiz, A.; Herranz, M. A.; Echegoyen, L. *J. Org. Chem.* **2005**, *70*, 5092.
(10) Cai, T.; Ge, Z. X.; Iezzi, E. B.; Glass, T. E.; Harich, K.; Gibson, H. W.; Dorn, H. C. *Chem. Commun.* **2005**, 3594.
(11) Cardona, C. M.; Kitaygorodskiy, A.; Echegoyen, L. *J. Am. Chem. Soc.* **2005**, *127*, 10448.
(12) Cardona, C. M.; Elliott, B.; Echegoyen, L. *J. Am. Chem. Soc.* **2006**, *128*, 6480.
(13) Rodriguez-Fortea, A.; Campanera, J. M.; Cardona, C. M.; Echegoyen, L.; Poblet, J. M. *Angew. Chem., Int. Ed.* **2006**, *45*, 8176.
(14) Cai, T.; Slebodnick, C.; Xu, L.; Harich, K.; Glass, T. E.; Chancellor, C.; Fettinger, J. C.; Olmstead, M. M.; Balch, A. L.; Gibson, H. W.; Dorn, H. C. *J. Am. Chem. Soc.* **2006**, *128*, 6486.
(15) Chen, N.; Zhang, E. Y.; Tan, K.; Wang, C. R.; Lu, X. *Org. Lett.* **2007**, *9*, 2011.
(16) Lukoyanova, O.; Cardona, C. M.; Rivera, J.; Lugo-Morales, L. Z.; Chancellor, C. J.; Olmstead, M. M.; Rodriguez-Fortea, A.; Poblet, J. M.; Balch, A. L.; Echegoyen, L. *J. Am. Chem. Soc.* **2007**, *129*, 10423.
(17) Chaur, M. N.; Melin, F.; Athans, A. J.; Elliott, B.; Walker, K.; Holloway, B. C.; Echegoyen, L. *Chem. Commun.* **2008**, 2665.
(18) Pinzon, J. R.; Zuo, T. M.; Echegoyen, L. *Chem.—Eur. J.* **2010**, *16*, 4864.
(19) To verify that the initial addition occurred at the [6,6]-junction, the same Prato reaction was carried out at lower temperature (110 °C), and the [6,6]-adduct was clearly observed as the major initial adduct.
(20) For details, see the Supporting Information (SI).
(21) Li, F. F.; Pinzon, J. R.; Mercado, B. Q.; Olmstead, M. M.; Balch, A. L.; Echegoyen, L. *J. Am. Chem. Soc.* **2011**, *133*, 1563.
(22) For details of the assignment, see the SI.
(23) Yang, S. F.; Popov, A. A.; Dunsch, L. *Angew. Chem., Int. Ed.* **2008**, *47*, 8196.
(24) Stevenson, S.; Lee, H. M.; Olmstead, M. M.; Kozikowski, C.; Stevenson, P.; Balch, A. L. *Chem.—Eur. J.* **2002**, *8*, 4528.
(25) Echegoyen, L.; Chancellor, C. J.; Cardona, C. M.; Elliott, B.; Rivera, J.; Olmstead, M. M.; Balch, A. L. *Chem. Commun.* **2006**, 2653.
(26) Stevenson, S.; Phillips, J. P.; Reid, J. E.; Olmstead, M. M.; Rath, S. P.; Balch, A. L. *Chem. Commun.* **2004**, 2814.
(27) Chen, N.; Pinzon, J. R.; Echegoyen, L. *ChemPhysChem* **2011**, *12*, 1422.
(28) The HPLC peak areas for the [5,6]- and [6,6]-adducts of $Gd_3N@C_{80}$ provided a 60:40 ratio, which was adjusted to 50:50 on the basis of the difference in the adducts' OD_{390} values (see Figure S56).
(29) Liu, T. X.; Wei, T.; Zhu, S. E.; Wang, G. W.; Jiao, M. Z.; Yang, S. F.; Bowles, F. L.; Olmstead, M. M.; Balch, A. L. *J. Am. Chem. Soc.* **2012**, *134*, 11956.
(30) Chaur, M. N.; Melin, F.; Ortiz, A. L.; Echegoyen, L. *Angew. Chem., Int. Ed.* **2009**, *48*, 7514.